Soil-Structure Interaction Effects on the Seismic Response of Multi-Span Viaducts

Sandro Carbonari, Michele Morici
Università Politecnica delle Marche. Dipartimento di Ingegneria Civile, Edile e dell'Architettura. Via Brecce Bianche, 60131 Ancona.

Francesca Dezi
Università di San Marino. Dipartimento di Economia e Tecnologia. Via Salita alla Rocca 44, 47890 San Marino città, Repubblica di San Marino.

Graziano Leoni
Università di Camerino. Scuola di Architettura e Design. Viale della Rimembranza, 63100 Ascoli Piceno.

Keywords: Bridges; Nonlinear behaviour; Soil-structure interaction; Substructure approach

ABSTRACT
The paper focuses on the effects of soil-structure interaction in the seismic response of multi-span viaducts on pile foundations. Analyses are performed by means of the substructure approach: the soil-foundation systems are studied in the frequency domain to obtain the foundation input motion and the dynamic impedance functions; inertial interaction analyses are carried out in the time domain accounting for the material nonlinear behaviour. Suitable lumped parameter models are introduced to simulate the frequency dependent behaviour of the soil-foundation system. A specific procedure for selecting and scaling real ground motions is proposed and used for the definition of the spatial seismic input. The seismic response of bridges on compliant base is compared with that obtained from fixed base analyses discussing the significance of soil-structure interaction effects.

1 INTRODUCTION

Seismic design of bridges are generally performed by assuming piers fixed at the base and synchronous seismic motions, defined on the basis of local hazard and soil classification. Actually, earthquake ground motion may be strongly different among the supports, especially for long bridges, due to both travelling effects, loss of coherency and local soil conditions that may modify the earthquake intensity and frequency content to such an extent that code spectra become not conservative. Furthermore, the compliance of the soil-foundation system may modify sensibly the response of a fixed base system. Bridge foundations interact with the surrounding soil and the superstructure producing a modification of the free-field seismic motion (kinematic interaction) and dissipating a part of energy from superstructure (inertial interaction).

This paper deals with the effects of Soil-Structure Interaction (SSI) on the seismic response of multi-span bridges founded on piles and reports the results obtained from an extension of the research undertaken in the framework of PRIN 2008, granted by the Italian Government.

Analyses are performed with a comprehensive methodology accounting not only for the filtering effect and the compliance of the soil-foundation system but also for site effects that are evaluated with specific site response analyses in which the soil nonlinear behaviour and the bi-directional nature of the seismic action are taken into account.

The analysis methodology exploits advantages of the substructure approach: the soil-foundation systems are analysed in the frequency domain with the numerical procedure of Dezi et al. (2009), which allows obtaining the dynamic impedance functions and the foundation input motion once the free-field motion is known. The seismic input is defined at the outcropping bedrock and an iterative propagation analysis is performed to guarantee, at the deposit surface, compatibility between the earthquake and code spectral accelerations evaluated at the bridge fundamental period. Both the current earthquake spectrum and the reference one are defined taking into account the two perpendicular horizontal components of the input motion. This procedure is different to that adopted in Carbonari et al. (2012); it avoids results scattering due to the nonlinear behaviour of the deposit and allows focusing on the effects of SSI due to the compliance of the soil-foundation system.

Bridges characterised by ductile and non-ductile behaviours are considered and designed with a Direct Displacement Based Approach (DDBA) (Priestly et al., 2007). The seismic response of bridges on compliant and fixed base is determined with nonlinear dynamic analyses by adopting a distributed plasticity model and introducing suitable Lumped Parameter Models (LPMs) at the piers base to account for the frequency dependent behaviour of the soil-foundation systems.

Results obtained from fixed and compliant base models are compared discussing effects of SSI on the response of bridges.

2 CASE STUDIES

A set of 10-span viaducts having different span length (25, 50 and 75 m) and pier height (10, 15 and 25 m) are considered (Figure 1a). The composite twin-girder deck is continuous and is constituted by a 12 m wide slab, with mean thickness of 0.30 m, sustained by two 6 m spaced steel I-shaped girders (Figure 1b). The vertical loads for the seismic combination are estimated to be about 140 kN/m including self-weights. The deck is supported on fixed bearings at the middle pier and on bearings fixed only in the transverse direction at the other piers; lock-up devices are adopted in the longitudinal direction to allow free elongations at service conditions; finally, multi-directional bearings are used at the abutments. Such a scheme has been chosen to have a system not affected by a double-path mechanism involving the deck as seismic resistant component.

A 40 m thick single layer soil deposit (Figure 2a) constituted by normally consolidated clays with properties reported in Figure 2c is considered. The deformable layer overlays a horizontal bedrock characterized by shear wave velocity $V_{s,b}$ = 800 m/s and density ρ_b = 2.2 Mg/m^3. Such a profile can be classified as a type D soil and has been selected to emphasise the effects of SSI; the non-synchronous input motions at the pier bases, due to loss of coherence of the earthquake signals, is neglected.

2.1 *Seismic design of piers*

In consideration of the deck restraint system, the seismic design is performed by considering the isolated piers on fixed base. Concrete C35/45 and steel grade B450C are adopted. The DDBA (Priestly et al., 2007) is used to design the bridge by imposing different ductility demands at Ultimate Limit State (ULS): piers with 2.4 m diameter and 25, 15 and 10 m high have been designed to achieve the ductility demand $\mu \approx 1$ (elastic behaviour) $\mu \approx 2$ and $\mu \approx 4$, respectively.

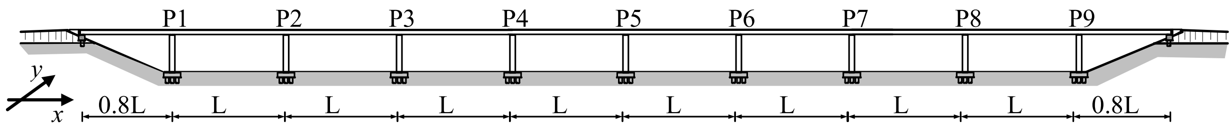

(a)

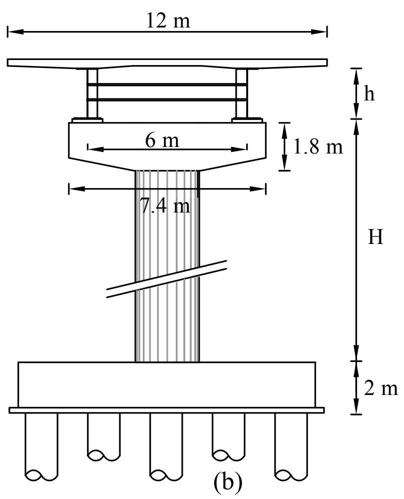

(b)

Case Studies	L [m]	H [m]	h [m]	H/D [m]	Δ_y [m]	Δ_d [m]	μ
H10L25	25	10	1.0	4.17	0.080	0.327	≈4
H15L25	25	15	1.0	6.25	0.175	0.358	≈2
H25L25	25	25	1.0	10.4	0.476	0.470	≈1
H10L50	50	10	1.9	4.17	0.080	0.327	≈4
H15L50	50	15	1.9	6.25	0.175	0.358	≈2
H25L50	50	25	1.9	10.4	0.476	0.470	≈1
H10L75	75	10	2.6	4.17	0.080	0.327	≈4
H15L75	75	15	2.6	6.25	0.175	0.358	≈2
H25L75	75	25	2.6	10.4	0.476	0.470	≈1

(c)

Figure 1. (a) Lateral view of the viaducts; (b) pier elevation and (c) geometric and design parameters of the case studies

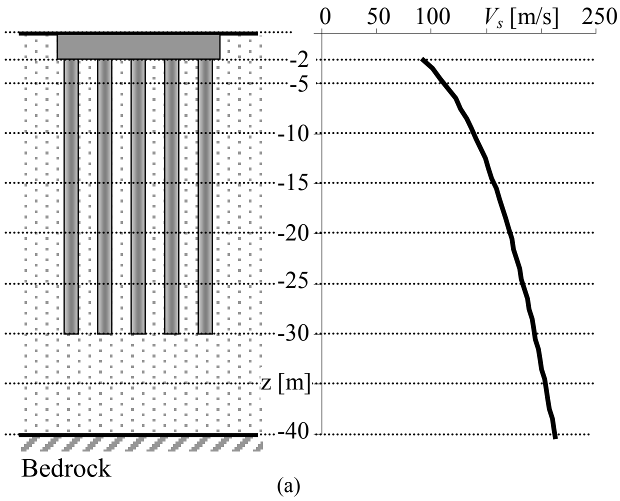

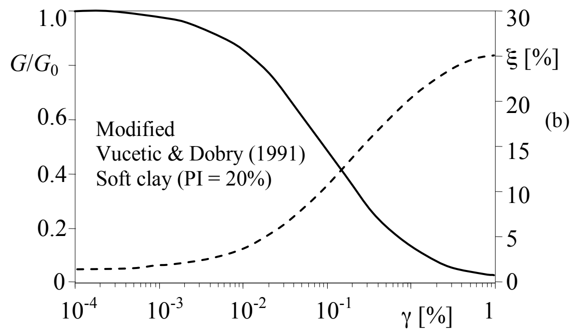

Mass density	1.83	[Mg/m^3]	(c)
PI	20	[%]	
Friction angle	28	[°]	
Undrained resistance	$0.35 \cdot \sigma'_{v0}(z)$	[kPa]	

Figure 2. (a) Soil profile and V_s profile; (b) normalized shear modulus and damping ratio curves (c) soil mechanical properties

Table 1. Longitudinal ρ_l and transverse ρ_w reinforcement ratios

Case Study	ρ_l [%]	ρ_w [%]
H10L25	1.00 (0.47)	0.62 (0.23)
H15L25	1.00 (0.44)	0.29 (0.16)
H25L25	1.00 (0.78)	0.29 (0.15)
H10L50	1.00 (0.97)	0.76 (0.40)
H15L50	1.00 (0.92)	0.30 (0.27)
H25L50	1.28	0.29 (0.22)
H10L75	1.53	0.98 (0.55)
H15L75	1.56	0.76 (0.40)
H25L75	2.06	0.76 (0.32)

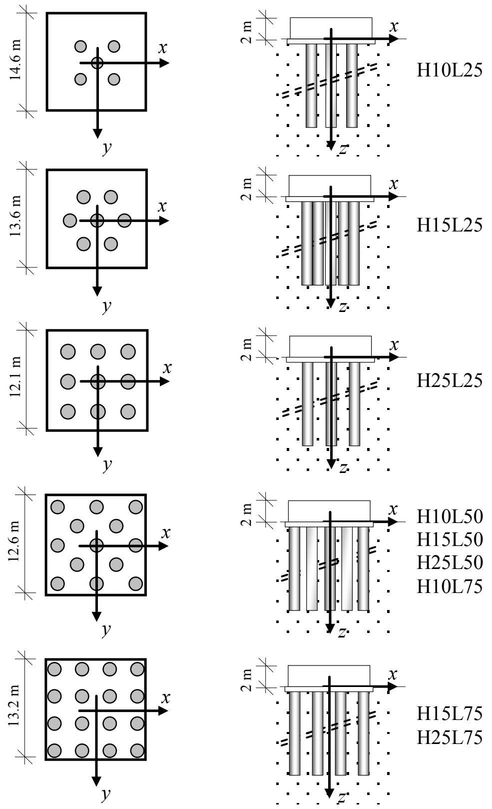

Figure 3. Pile group foundations

The soil type D elastic displacement response spectrum defined by the EN 1998-1 (2004) is adopted by considering a Peak Ground Acceleration (PGA) of 0.47g (corresponding to a PGA of 0.35g for soil type A). The "30%-rule" is used to account for the bi-directional seismic action.

The shear failure is prevented by means of a suitable capacity design. Reinforcement ratios (Table 1) and detailing of structural elements comply with provisions of NTC2008; amounts of reinforcements required for the element resistance are reported in brackets if lower than minimum values.

2.2 Seismic design of foundations

Foundations are constituted by groups of bored concrete piles with diameter $d = 1200$ mm, spacing $i = 3d$ and length $l = 30$ m. Foundations of piers are designed according to hierarchy principles in order to avoid the pile plasticization. Five different foundations have been considered for the nine bridges (Figure 3). As a consequence of the high seismicity level and the poor soil properties, a considerable number of piles is necessary in some cases to withstand the lateral actions that produce significant eccentricities of loads. For this purpose, depending on the case study, a certain amount of the bearing capacity of the foundation is entrusted to the rigid cap.

3 SEISMIC INPUT

The seismic input for the spatial analyses of the considered bridges consists of a set of pairs of horizontal accelerograms. One peculiarity of the problem examined is that the motion due to waves travelling through the deposit must be imposed along the piles (kinematic interaction) when analysing effects of SSI. This raises the question on how to select and scale the accelerograms. To assess the behaviour of the bridges designed considering the spectrum for soil type D, a specific strategy has been adopted to avoid excessive scattering of the results due to the local response of the deposit: the accelerograms have been selected with reference to rock outcropping sites (soil type A) and scaled to achieve, at the deposit surface, the design spectral acceleration at the fundamental period of the bridges. This procedure is substantially different to that adopted in (Carbonari et al., 2012) where accelerograms were selected and scaled to guarantee the compatibility between their mean spectrum and the code one, for soil type A. In that case, results obtained were very scattered and for some accelerograms the response of the bridges were very different to the average response. The procedure here adopted is thus preferred as the objective of this work is to investigate the effects of SSI in terms of foundation soil compliance.

A second question regards how to scale the bidirectional soil shakings. In this case, establishing a single spectrum starting from spectral ordinates for the two horizontal components becomes a crucial issue with reference both to the selected ground motion and to the target spectrum. Different methods are available in the literature, such as the geometric mean spectrum, the arithmetic mean spectrum, or the square root of the sum of the squares spectrum (Beyer and Bommer, 2007). The various methods are affected by the directivity of the motion and the resulting spectrum is generally sensitive to the choice of the vectorial base used to describe the bidirectional accelerogram. In this work the geometric mean spectrum

$$Sa_{GMxy}(T) = \sqrt{Sa_x(T) \cdot Sa_y(T)} \quad (1)$$

is considered ($Sa_i(T)$ is the spectral component in the i-direction) since it has been demonstrated that the resulting spectrum is less sensitive to the orientation of the ground-motion axes than in the other definitions (Baker and Cornell 2006).

Seven ground motions, recorded on site class A, are thus selected (Iervolino and Cornell, 2005) from the European Strong Motion Database (Ambraseys et al., 2002) to represent the seismic shaking at the outcropping bedrock (Table 2). The earthquake are characterized by epicentral distances minor than 100 km and magnitude M_w greater than 6.0. The two orthogonal horizontal components of each ground motion are associated to the bridge longitudinal (x) and transverse (y) directions.

Site effects are captured by performing local response analyses in which the nonlinear soil behaviour is taken into account. With reference to each bridge, the evaluation of the shaking at the ground surface is carried out, for each record, by means of the following iterative procedure:

- correction of the as-registered ground motion (baseline and filtering);
- evaluation of the two components of the motion at the bedrock, starting from registrations at outcropping rock;
- one-dimensional local response analyses in the two separate directions and definition of the relevant surface motions;
- evaluation of the response spectra Sa_i ($i = x, y$) at the ground surface and calculation of the geometric mean spectrum Sa_{GMxy};
- comparison of the spectral acceleration of the geometric mean spectrum at the structural fundamental frequency with the relevant design code spectrum and, accordingly, scaling of the ground motion.

The fundamental mode T_1 of the superstructure is adopted. Furthermore, concerning local response analyses, the soil shear modulus degradation and damping are calibrated according to the modified curves of Vucetic and Dobry (1991) (Figure 2), taking into account the maximum shear strain level occurred during the bi-directional shaking. In particular, the maximum effective shear strain level is obtained from

$$\gamma_{max} = 0.65 \max\left(\sqrt{\sum_i \gamma_i(t)^2}\right) \quad (2)$$

where γ_i ($i = x, y$) is the i-th component of the shear strain, obtained in the propagation analysis.

In the case under examination, the profile of the shear modulus at low strains (G_0), from which the shear wave velocity is derived (Figure 2b), is obtained according to empirical formulas available in the literature (Calabresi and Manfredini, 1976; D'Onofrio and Silvestri, 2001); the values of $V_{s,30}$ (149 m/s) falls within the range defined by NTC2008 and EN 1998-1 (2004) for soil type D.

Figure 4 compares, for each case study, the obtained mean geometric displacement response spectra at the ground surface (grey lines) with the relevant design response spectrum (dotted line); the arithmetic mean spectrum (black line) obtained by averaging the individual geometric mean spectra is also reported. Since the soil has a nonlinear behaviour, amplification effects depend on the earthquake frequency content and on the scale factor necessary to achieve the target spectral ordinate; however, major site effects are evident, for the case studies, in the period range 1÷3 s. It can be observed that the arithmetic mean spectrum is able to represent the target code spectrum up to a period of about 1.5 s; for higher periods some discrepancies are evident.

4 SSI ANALYSIS

4.1 Kinematic interaction analysis

The analyses of the soil-foundation systems are performed by means of the numerical model proposed by Dezi et al (2009) which allows obtaining the FIM and the frequency-dependent foundation impedances necessary for the subsequent inertial interaction analyses. Piles are modelled by 1 m long finite elements and are supposed to have density $\rho_p = 2.5$ Mg/m³ and Young's modulus $E_p = 23500$ MPa to account for the concrete cracking.

As already discussed, the spatial variability of motion is neglected and the pile groups of Figure 3 are analysed to obtain the FIM to be considered at all the bridge supports. The bidirectional free-field motion within the deposit, obtained from the local response analyses, is used as input motion in the kinematic interaction analyses.

Figure 5 shows with continuous lines the non-null components of the impedance matrix for the pier foundation of viaducts H15L75 and H25L75.

Table 2. Selected records (E.C.: Earthquake Code; W.C.: Wavefront Code; S.C.: Station Code)

Earthquake (E.C.) (W.C.)	Station (S.C.)	Date [dd/mm/yy]	Δ [km]	Magnitude [Mw]	PGA (x) [m/s^2]	PGA (y) [m/s^2]
Friuli (34) (55)	Tolmezzo Diga Ambiesta (20)	6/5/1976	23	6.5	3.097 (E/W)	3.499 (N/S)
Friuli - aftershock (65) (149)	Tarcento (26)	15/9/1976	12	6.0	1.103 (E/W)	1.339 (N/S)
Tabas (87) (182)	Dayhook (54)	16/09/1978	12	7.3	3.779 (N10E)	3.316 (N80W)
Kalamata (1885) (5819)	Koroni-Town Hall - Library (1321)	13/10/1997	48	6.4	1.146 (305)	1.185(035)
Strofades (1887) (5826)	Kyparrisia-Agriculture Bank (1323)	18/11/1997	90	6.6	0.723 (297)	0.647 (027)
Kozani (2029) (6100)	Kastoria-OTE Building (1315)	13/05/1995	50	6.5	0.194 (260)	0.182 (350)
Kozani (2029) (6174)	Veria-Cultural Center (1354)	13/05/1995	60	6.5	0.260 (026)	0.293 (158)

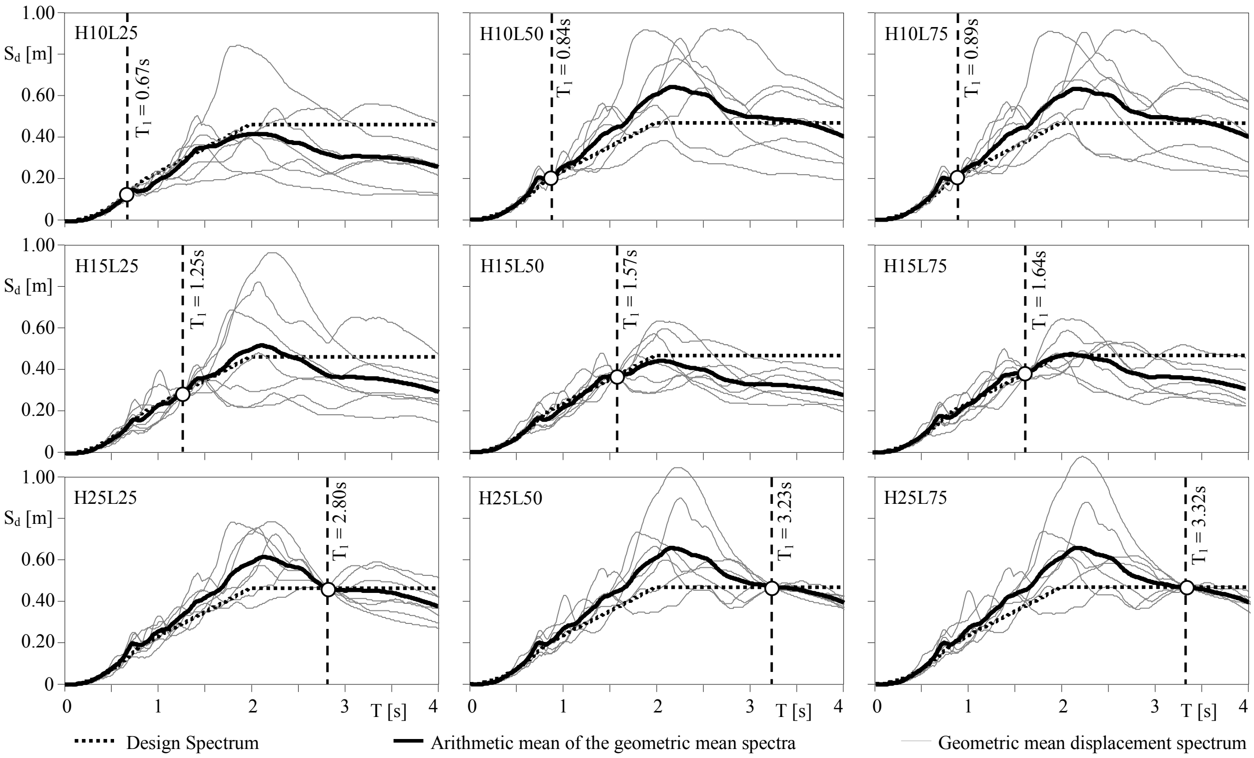

Figure 4. Single mean displacement response spectrum of the selected accelerograms compared with reference spectra

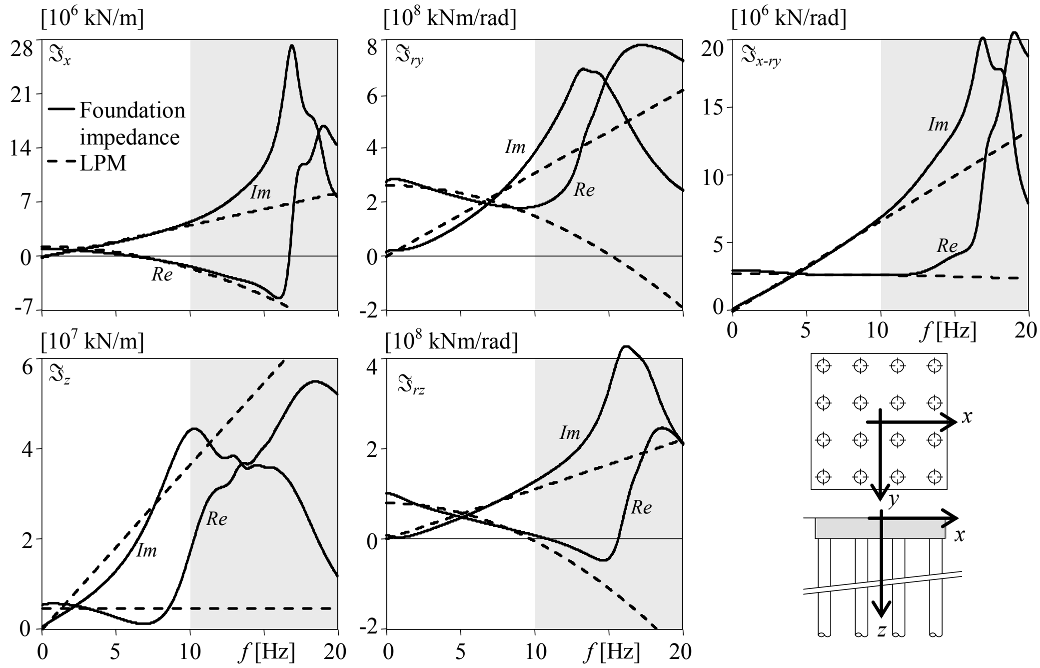

Figure 5. Non-null components of the impedance matrix of the soil-foundation system of viaducts H15L75 and H25L75

4.2 *Inertial interaction analysis*

The nonlinear inertial interaction analyses of the viaducts must be carried out by considering frequency dependent compliant restraints at the base of piers, in order to capture both the compliance and the radiation damping of the soil-foundation system. However, since analyses must be performed in the time domain suitable LPMs, constituted by assemblages of masses, springs and dashpots (Wolf, 1988), are adopted to simulate the foundation behaviour. The LPM shown in Figure 6 is used herein; the 25 constants are calibrated with a least squares procedure in order to achieve the better approximation of the foundation impedance functions in the frequency range 0÷10 Hz; examples of impedances of the LPM are shown in Figure 5 with dashed lines together with the real impedances of the soil-foundation system.

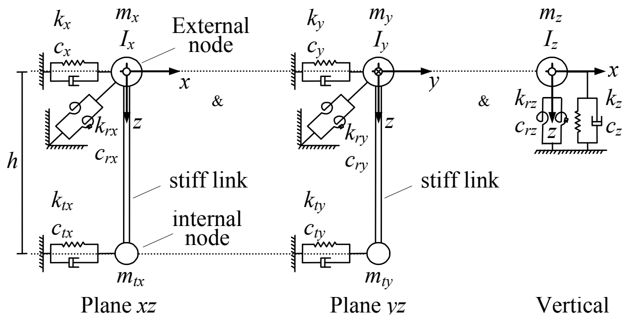

Figure 6. Adopted LMP

LPMs are implemented in the three-dimensional finite element models of the viaducts developed in Seismostruct (2007). Besides the Compliant Base (CB) models, obtained by introducing the LPMs, Fixed Base (FB) models, fully restrained at the base of piers, are also considered. In both CB and FB models, beam elements with a linear elastic behaviour are used for the steel-concrete composite deck, accounting for the change of steel plate thicknesses along the deck and for the concrete cracking in the evaluation of the element mechanical properties. Piers are modelled with fiber elements in order to capture their nonlinear behaviour under bi-directional motions; Mander's laws (1988) are considered for the confined and unconfined concrete while the constitutive model of Menegotto and Pinto (1973) is used for the reinforcement. Rigid links are suitably adopted to model the eccentricity between the pier and deck centroids. Furthermore, 5% structural damping is introduced in terms of tangent stiffness proportional damping.

5 RESULTS

In this section the effects of the SSI on the nonlinear seismic response of the bridges are discussed by comparing results of the CB models with those obtained from the FB models. Unless otherwise specified, results refer to the mean values obtained from the nonlinear dynamic analyses performed with the set of real accelerograms.

5.1 *Structural displacements and ductility demands*

Structural displacements represent important performance parameters due to their strong correlation with damage. Figure 7 shows the maximum modulus of the relative displacements of the top of piers (i.e. measured with reference to the foundation cap). The design displacement (dashed lines), as well as the displacement thresholds corresponding to the nominal yielding of the pier base cross sections (dotted lines), are reported. It can be observed that, with reference to FB structures, the maximum mean displacements of bridges H15L# are in good agreement with the design ones while for the remaining bridges same differences are evident; these are more pronounced in the case of bridges H10L25 and H10L75.

Increments of the deck displacements due to SSI can only be observed in the case of bridges with more rigid piers (H10L#) and in the case of bridge H15L25 for which the short span length

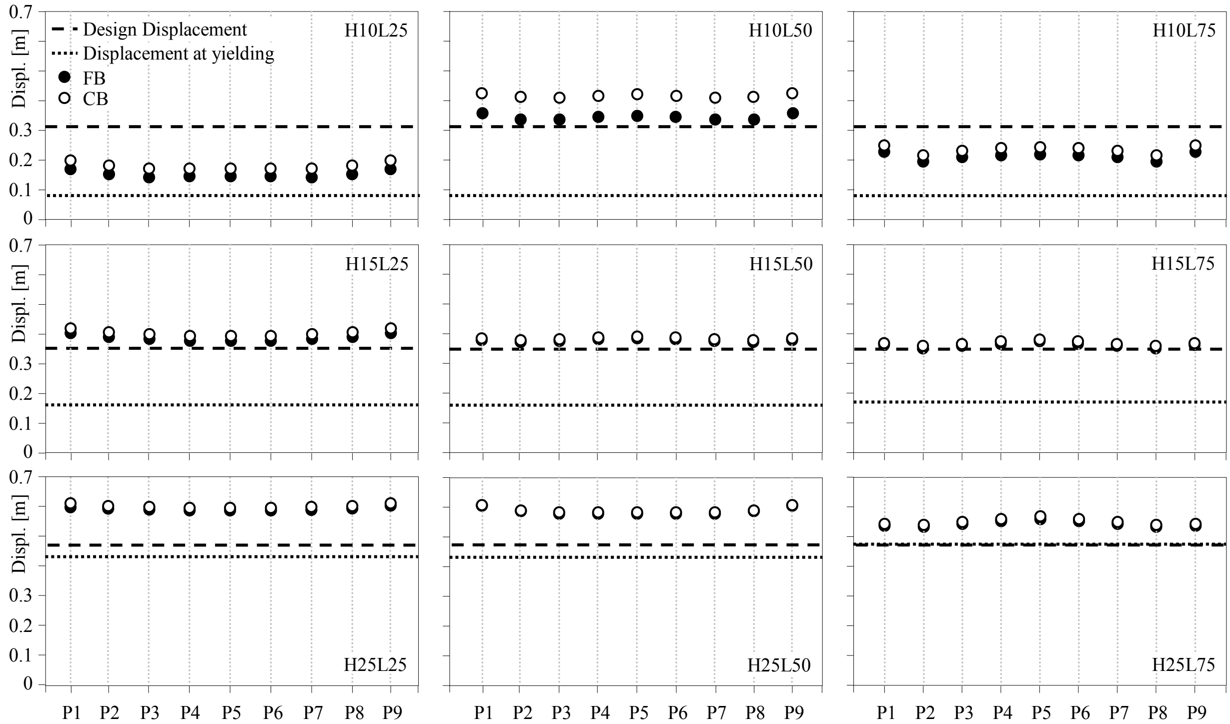

Figure 7. Maximums relative displacement at the top of the piers

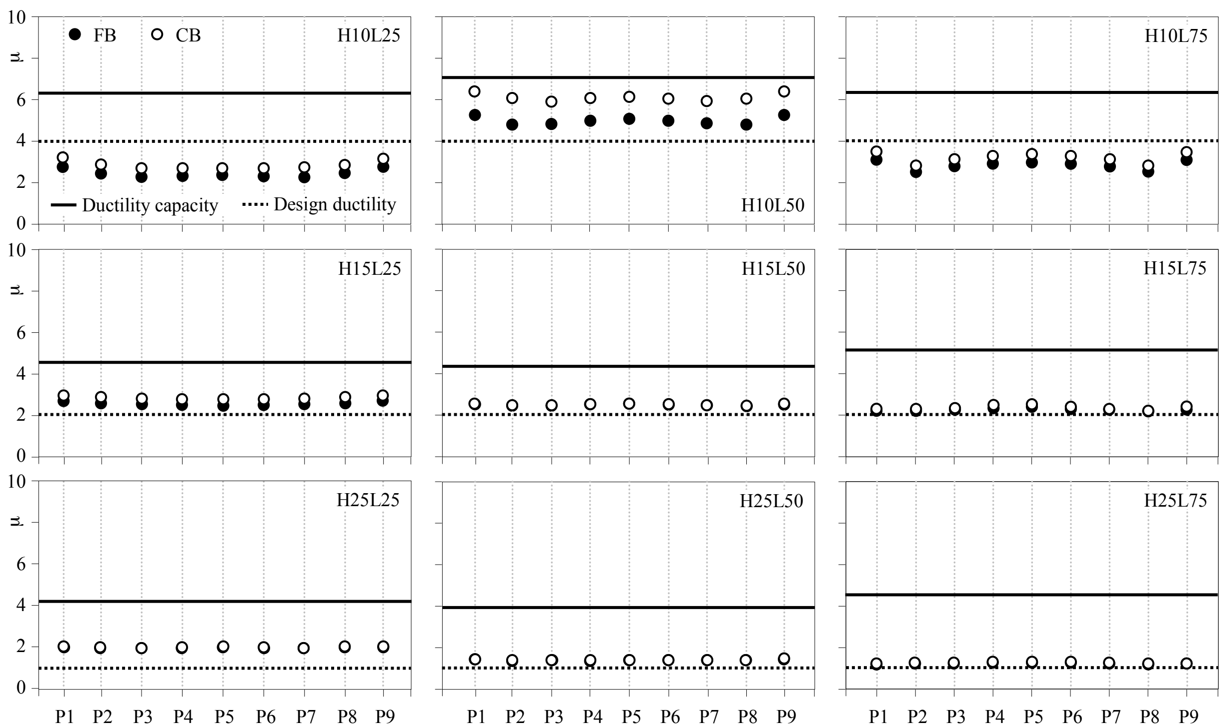

Figure 8. Displacement ductility demand

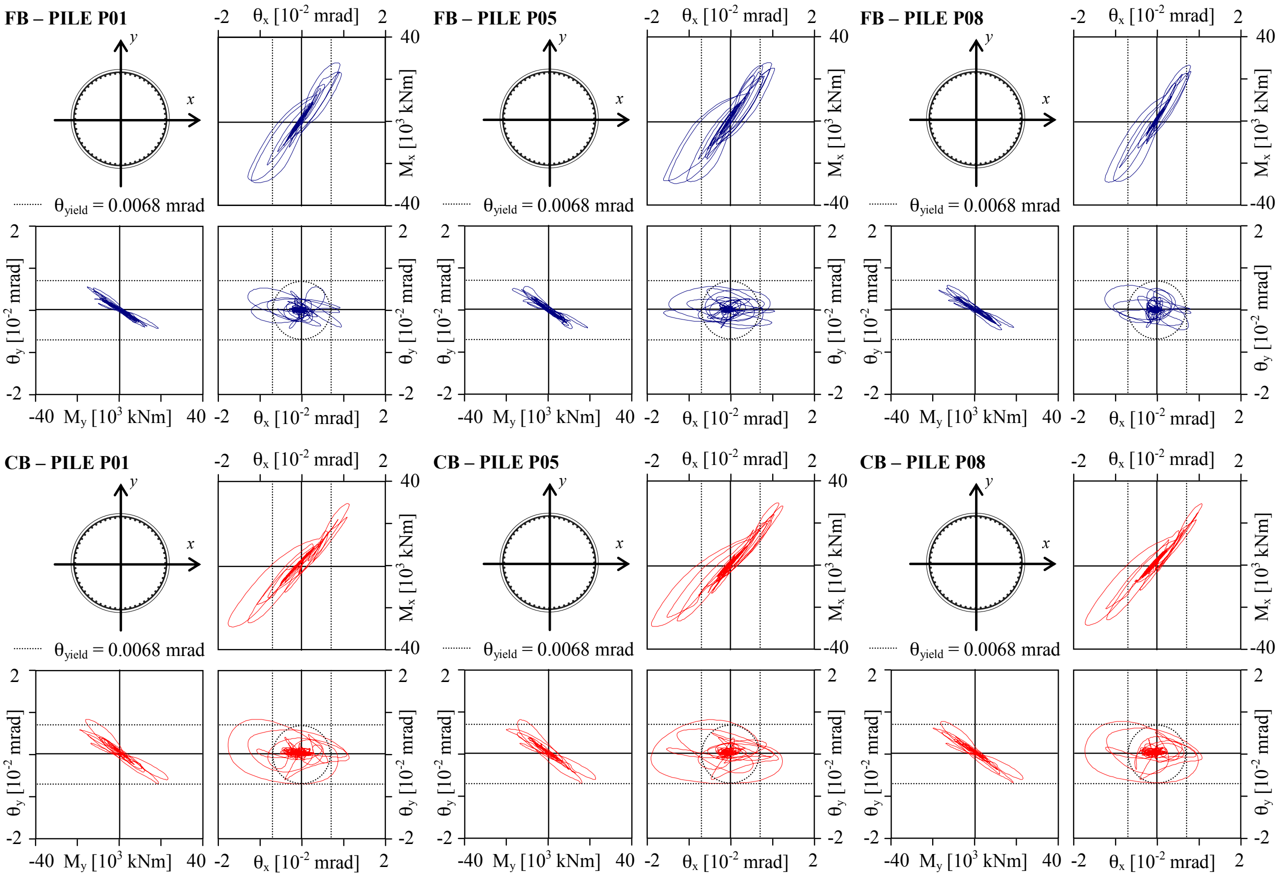

Figure 9. Moment-Rotation diagrams of piers P1, P5 and P8 for the Friuli earthquake for Bridge H15L50

contributes to laterally stiffen the pier; for the remaining bridges SSI affects slightly the maximum deck displacements.

Finally, it is worth to observe that the displacements are slightly different at the various piers due to the interaction induced by the continuous deck. This effect is obviously more pronounced for the longest bridges (H#L75).

Figure 8 compares the ductility demand of each pier with the relevant capacity. Concerning the CB models, the effects of the foundation rigid rotation are suitably subtracted. Consistently with observations on displacements, the ductility demand of piers is almost coincident with the design one in the case of bridges H15L# whereas for the remaining bridges same discrepancies are evident. SSI increases the displacement ductility demand of piers of bridges H10L#, as a consequence of the displacement increase; in the case of bridge H10L50 the ductility demand of lateral piers is very close to the capacity.

5.2 Piers plastic hinges rotation demands

In Figure 9 the moment-rotation curves of the base cross sections of piers P1, P5 and P8 of bridge H15L50, obtained from both the CB and FB models subjected to the Friuli earthquake (Tolmezzo Diga Ambiesta), are reported. In particular, moment-rotation curves M_x-θ_x and M_y-θ_y are reported in separate plots and related to the time history of rotations, in the plane θ_y-θ_x. With reference to the FB model, an increase of the plastic hinge rotation demand is observed as a consequence of SSI.

Figure 10 shows the rotation demands of plastic hinges at the base of piers, obtained by averaging results of the analyses performed on FB and CB models. In the graphs, the yielding (θ_y) and the ultimate (θ_u) rotations calculated as suggested by EN 1998-2 (2005) by adopting the probable material properties are also reported; a safety factor $\gamma_{R,p}$ = 1.4 is applied to the ultimate plastic rotation. These depend on the ultimate cross section curvature (that increases with the amount of reinforcement and by reducing the piers height and the span length, as a consequence of the axial force reduction), and on the plastic hinge length and yield rotation (that decrease with the pier height).

Consistently with above observations concerning displacements and ductility, SSI increases the rotation demand of plastic hinges primarily for piers of bridges H10L#; in particular for the case H10L50 the demand are close to the rotation capacity.

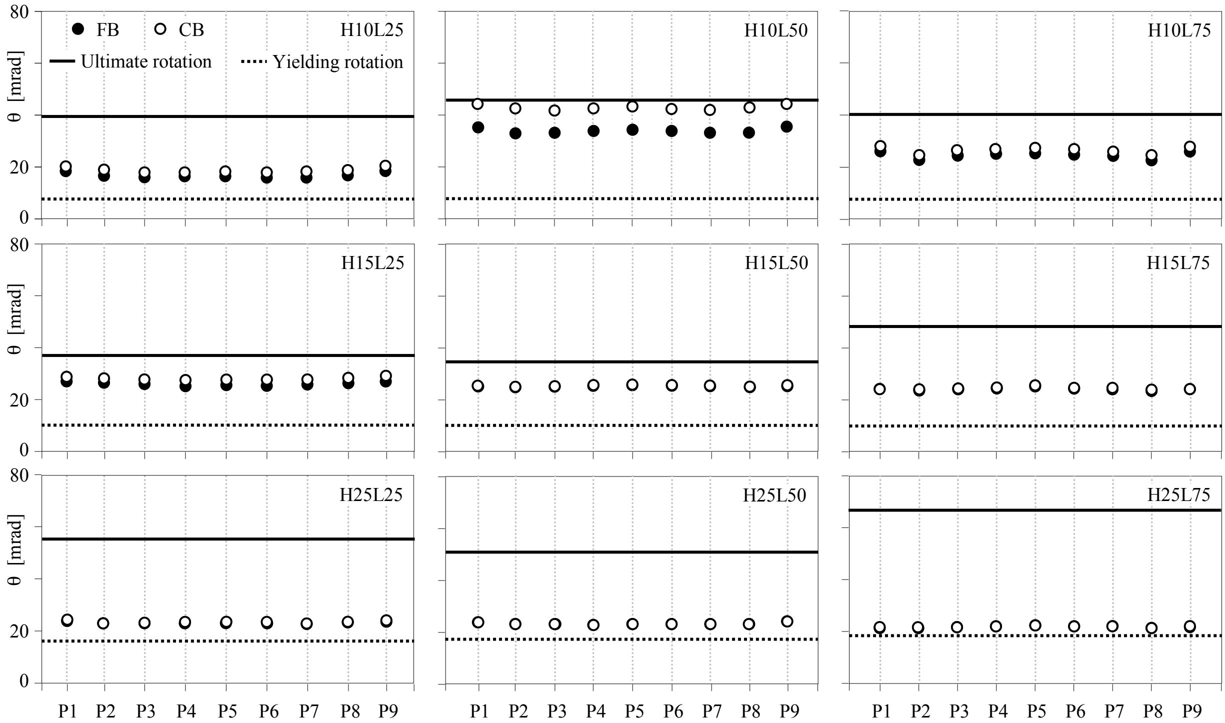

Figure 10. Rotation demands and capacity of plastic hinges

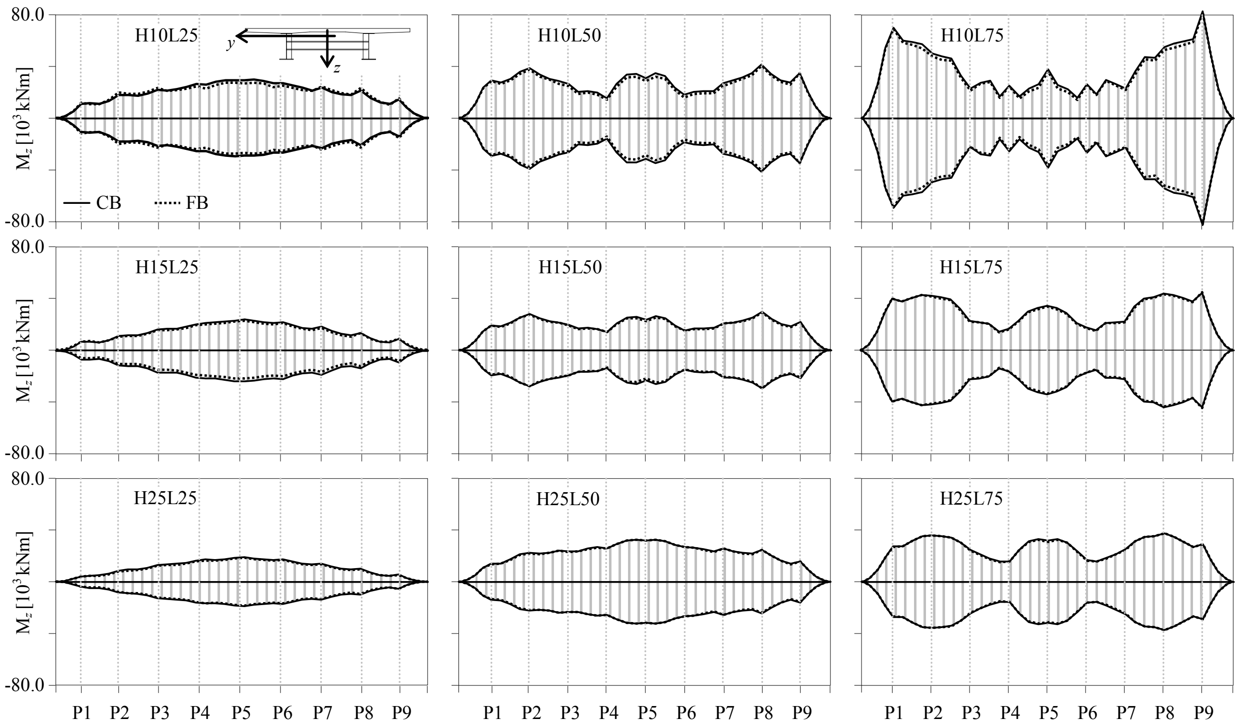

Figure 11. Deck transverse bending moments

5.3 *Deck transverse bending moments*

Figure 11 shows the transverse bending moments of the deck obtained from the analyses of the FB and CB models. Stress resultants increase by reducing the piers height as a consequence of the higher stiffness of the substructures and of the differential displacements of the pier. Furthermore, with reference to bridges with span length greater than 50 m, two pinchings of the bending moment envelopes are evident; these are due to the increasing contribution of the superior modes of the flexible decks. Middle spans are characterised by bending moments of the same order of magnitude, independently on the pier height, while bending moment in lateral spans increases by reducing the pier height and increasing the span length. SSI effects on the deck bending moments are negligible.

Finally, as expected in consideration of the restraint layout that foresees multidirectional bearings at the abutments, the magnitude of the stress resultants are much lower than the deck yielding moment.

CONCLUSION

SSI effects on the seismic response of multi-span viaducts on pile foundations have been investigated. Bridges characterised by ductile and non-ductile behaviours are considered. A specific procedure for the selection and scaling of ground motions is proposed and used for the definition of the spatial seismic input. In particular, real accelerograms characterised by two horizontal components at the outcropping bedrock are adopted; an iterative local response analysis is thus performed accounting for the soil nonlinear behaviour; the mean geometric response spectrum is considered to combine the two components of the motion at the ground surface and to check the compatibility with the design spectrum.

The seismic response of the bridges on compliant base is compared with that obtained from fixed base analyses discussing the significance of SSI effects. Results demonstrate that, despite bridges are founded on a very soft soil, SSI does not play a significant role in the definition of the structural response. Increases of about 15% of the maximum deck displacements have been observed only in the case of stiff piers. However in such cases the plastic hinge rotation demand may increase to such an extent that the maximum capacity may be attained.

ACKNOWLEDGMENT

This research is an extension of the research undertaken in the framework of PRIN 2008 granted by the Italian Government and coordinated by professor Camillo Nuti. The soil deposit and the foundations were chosen and designed by the local research unit of the University of Naples “Federico II” coordinated by professor Francesco Silvestri.

REFERENCES

Ambraseys, N., Smit, P., Sigbjornsson, R., Suhadolc, P. and Margaris, B., 2002. Internet-Site for European Strong-Motion Data, European Commission, Research-Directorate General, Environment and Climate Programme.

Baker, J. W. and Cornell, A., 2006. Correlation of response spectral values for multicomponent ground motions, *Bulletin of the Seismological Society of America* **96**, 215–227.

Beyer, K., Bommer, J.J., 2007. Selection and Scaling of Real Accelerograms for Bi-Directional Loading: A Review of Current Practice and Code Provisions. *Journal of Earthquake Engineering* **11**, 13–45.

Calabresi, G. and Manfredini, G., 1976. Terreni poco consistenti in Italia. *Rivista Italiana di Geotecnica*. **10**(1), 49-64.

Carbonari, S., Morici, M., Dezi, F., Nuti, C., Silvestri, F., Tropeano, G. and Vanzi, I., 2012. Seismic response of viaducts accounting for soil-structure interaction. 15 WCEE – The 15th World Conf. on Earthquake Engng, Lisbon, Portugal, 24-28 Sept. 2012, paper n.4150.

D’Onofrio, A. and Silvestri, F., 2001. Influence of micro-structure on small-strain stiffness and damping of fine grained soils and effects on local site response. IV Int. Conf. on 'Recent Advances in Geotech. Earthquake Engng and Soil Dynamics'. S. Diego, CA. Paper 1.19.

Dezi, F., Carbonari, S. and Leoni, G., 2009. A model for the 3D kinematic interaction analysis of pile groups in layered soils. *Earthquake Engng Struct. Dyn*. **38**(11), 1281-305.

EN 1998-1, 2004 Eurocode 8: Design of structures for earthquake resistance - Part 1: General rules, seismic actions and rules for buildings.

EN 1998-2, 2005 Eurocode 8: Design of structures for earthquake resistance - Part 2: Bridges.

Iervolino, I. and Cornell, C., 2005. Record selection for nonlinear seismic analysis of structures, *Earthquake Spectra* **21**(3), 685–713.

Mander, J.B., Priestley, M.J.N. and Park R., 1988. Theoretical Stress-Strain Model for Confined Concrete. *Journal of Structural Engineering ASCE*. **114**(8), 1804-826.

Menegotto, M., and Pinto, P.E., 1973. Method of analysis for cyclically loaded R.C. plane frames including changes in geometry and non-elastic behaviour of elements under combined normal force and bending. Symposium on the Resistance and Ultimate Deformability of Structures Acted on by Well Defined Repeated Loads, Zurich, Switzerland, 15-22.

NTC2008, 2008. Technical rules for constructions. (in Italian).

Priestley, M.J.N., Calvi, G.M., Kowalsky, M.J., 2007. *Displacement-Based Seismic Design of Structures*, IUSS Press, Pavia, Italia.

SeismoSoft, SeismoStruct. (2007). A computer program for static and dynamic nonlinear analysis of framed structures, available from URL: http://www.seismosoft.com.

Vucetic, M. and Dobry, R., 1991. Effect of soil plasticity on cyclic response. *Journ. of Geot. Eng. ASCE*. **117**(1), 89-107.

Wolf, J.P., 1988. *Soil-structure interaction analysis in time domain*, Prentice-Hall, Englewood Cliffs, N.